A transient pressure pulse method for the measurement of permeability of a cement grout

A.P.S. Selvadurai and P. Carnaffan

Abstract: The paper discusses the application of a transient pressure pulse technique for the laboratory evaluation of the permeability characteristics of a cementitious grout material with a relatively low permeability. The experimentation involves the internal pressurization of a cylindrical grout specimen with a concentric circular cavity. The time-dependent decay of the fluid pressure within the cavity is used as the basis for the computation of the permeability of the grout. The paper presents details of the experimental methodologies and the mathematical procedures which are used to evaluate the permeability. The results of a series of radial flow pressure pulse tests are used to ascertain the permeability characteristics of a cementitious grout.

Key words: permeability, pulse tests, cement grout, transient tests, laboratory tests.

Résumé : L'article examine l'application de la technique d'impulsion de pression transitoire pour l'évaluation en laboratoire des caractéristiques de perméabilité d'un coulis de ciment à perméabilité relativement faible. Les essais impliquent la mise en pression interne d'un échantillon cylindrique de coulis de ciment à cavité concentrique circulaire. La réduction de la pression du fluide dans la cavité en fonction du temps a été utilisée comme base pour calculer la perméabilité du coulis. L'article présente en détail les méthodes expérimentales ainsi que les calculs mathématiques utilisées pour évaluer la perméabilité. Les résultats d'une série d'essais d'impulsion de pression d'écoulement radial ont été utilisés pour déterminer les caractéristiques de perméabilité du coulis de ciment.

Mots clés : perméabilité, essais d'impulsion, essais transitoires, essais de laboratoire.
[Traduit par la Rédaction]

1. Introduction

Permeability can be defined as that property of a porous material which governs the rate at which fluid moves through the pore structure. The terms absolute permeability and intrinsic permeability are often used to describe the permeability, K, of a porous medium which is independent of the properties of the fluid migrating through the pore structure. The units associated with permeability are length squared (e.g., m^2 or ft^2). The term hydraulic conductivity, k, describes the ease with which a specific fluid migrates through a porous medium. The units associated with hydraulic conductivity are length per unit time (e.g., m/s or ft/s). Occasionally, the term permeability has unfortunately been used to refer to the hydraulic conductivity of a porous material with respect to a specific fluid. Throughout this paper the term permeability will be used to signify the absolute permeability.

The need for the accurate estimation of the permeability characteristics of cementitious materials such as concretes and grouts is dictated by considerations of the durability of civil engineering facilities. Concrete constitutes the bulk of structures such as buildings, bridges, roadways, dams, pipes, earth retaining structures, and water storage structures. The importance of the permeability characteristics of concrete becomes quite evident in applications such as pipes, sewers, and water retaining structures where the permeability must be sufficiently low to prevent visually detectable leakage out of water retaining structures or groundwater influx into nonpressurized pipes. In purely "structural" applications, an important function of the concrete is to provide protection to the reinforcing steel. Permeability is identified as one key property that influences the durability of concrete, which in turn protects reinforcing steel from corrosion. The importance of permeability has reemphasized the suggestion that in the specification of concrete durability, the governing criteria should be based on considerations of the permeability of concrete and the diffusion of chemicals through concrete rather than on the traditional criteria which are solely based on considerations of strength (Dhir and Byars 1993). The resistance of concrete to damage from freezing and thawing can be dependent on the permeability of the cement paste. Deterioration of concrete due to freeze–thaw action can be attributed to hydraulic pressures generated within the cement paste and (or) within the aggregate as unfrozen water is displaced during expansion of water during freezing. It is therefore important for concrete materials to possess permeability characteristics which will inhibit saturation of the pores so that expansion-induced displacement of water does not create adverse stresses within the microstructure of the concrete.

In recent years, the use of cement grouts has been advocated

in geo-environmental endeavours. The deep geological disposal of heat-emitting nuclear fuel wastes requires the assessment of permeability characteristics of both concrete and natural geological materials such as rocks. For example, the irradiated heat emitting spent fuel from CANDU reactors is currently stored in water pools in concrete bays. Even at this stage the permeability characteristics of concrete are important to the safety of the temporary storage (Lyon 1980; Dixon and Rosinger 1984; Wright 1991). In the Canadian context, the long-term disposal of such heat-emitting waste calls for the construction of deep vaults in granitic rock formations in the Canadian Shield. Although a series of multiple engineered barriers (e.g., metallic waste containers and engineered clay barriers) are to be used in such repositories, the natural geological barrier plays an important role in attenuating any long-term effects of radionuclide migration (Laughton et al. 1986; Lopez 1987; OECD 1988; Pusch 1990; Johnson 1994). Since natural fractures in geological media form the primary pathways for radionuclide migration, cement grouts have been proposed as agents for sealing fractures particularly in the vicinity of the repository (Gray 1993). The permeability characteristics of the cement grout and that of the interface between grout and the natural rock are therefore of critical importance to the waste disposal concepts. In other applications, it is proposed that the containers that house low-level radioactive wastes could be encapsulated in concrete. The efficiency of this dry storage scheme will thus be influenced by the permeability characteristics of the concrete. Figure 1 presents a summary of the category of problems where the permeability of concrete becomes important to the successful engineering design of civil engineering facilities.

2. Factors affecting permeability

Although permeability is considered to be purely a material property, there are several factors other than the test material that can influence its measured values. These factors include the state of stress in the sample, chemical effects, the degree of saturation, and the characteristics of the permeating fluid. These factors can change the measured permeability of a sample by several orders of magnitude.

The state of stress within the sample can have a considerable influence on the permeability of a porous material. Large stress (i.e., stresses such as those found deep in the earth or within the core of a concrete dam) can cause deformation of the pore skeleton, possibly inducing closure of small interconnected cracks or reducing the pore volume. Brace et al. (1968) conducted tests on samples of Westerly granite, which were subjected to confining pressures as large as 400 MPa, and observed that permeabilities reduced from 3.5×10^{-19} m^2 at 5 MPa to 3.9×10^{-21} m^2 at 400 MPa. Knutson and Bohor (1963), Bernaix (1966), Kranz et al. (1979), and Heystee and Roegiers (1981) have also observed reductions in the permeability due to large confining pressures. Heystee and Roegiers (1981) have also observed increases in permeability in rock specimens that are subjected to tensile stresses.

The permeating fluid and the test sample can chemically react. The permeating fluid can dissolve and leach out minerals or the permeant can deposit minerals on the pore skeleton. In a test environment, this can usually be avoided by selecting a chemically inert permeating fluid. Chemical effects are par-

ticularly difficult to control when testing cement paste samples because of the continued hydration process in the cement paste. Water migrating through the matrix during the test can react with the unhydrated cement particles to alter the pore structure of the cement. This hydration process can result in the alteration of the pore space or between particles. The reduction in the pore space can alter the fluid entry characteristics of the pore space.

An essential requirement of permeability testing is that the pore space must be fully saturated by the permeating fluid. In practice, this implies that for a water-based permeability test, all air within the communicating pores must be removed and replaced with water. The complete saturation process can be difficult and time consuming to achieve, particularly with large samples.

The viscosity (and compressibility) of the permeating fluid is accounted for in the calculations that determine the coefficient of permeability of a material. Therefore, in principle, it should not make a significant difference whether the permeating fluid is water, air, or kerosene. Studies have, however, shown that permeabilities determined using a gas as a permeating fluid (as opposed to a liquid) are almost always higher (Bamforth 1987; Ahmed et al. 1991). Gas permeabilities as much as 78.5 times that of water permeabilities have been reported by Bamforth (1987). The discrepancy between liquid and gas permeability measurements becomes larger as the permeability decreases. This discrepancy has been attributed to a phenomenon called gas slippage, also known as the Klinkenberg effect (Corey 1990; Ahmed et al. 1991). Gas slippage is the term used to describe the observation that a gas has a higher velocity near a grain surface than does a liquid. As a result, the quantity of gas flowing through a capillary is larger than that predicted by the classical Poisseulle flow equation (Bamforth 1987).

3. Measurement of permeability

Despite its long recognized engineering importance, there are no Canadian Standards Association (CSA) or American Society for Testing and Materials (ASTM) standardized tests, at least to the authors' knowledge, for measuring the permeability of concrete (Whiting and Walitt 1988; Roberts and Skalny 1989). Consequently, scientists and engineers have developed a variety of techniques for the measurement of properties related to permeability; these include water absorption tests (see, for example, Kay (1992)), gas permeability tests, and water permeability tests. Some of the tests currently in use do not directly measure the permeability of the concrete; they only give relative estimates for the permeability of a concrete, or an index number providing a qualitative assessment between different mix designs (e.g., concrete mix A is less permeable than concrete mix B).

It would seem clear that a standard test is therefore desirable in order that useful comparisons can be made between results for the purposes of evaluating permeabilities.

In general, all permeability tests can be classified either as laboratory testing techniques or as *in situ* testing techniques. *In situ* permeability testing techniques generally give a value of permeability that is representative of the overall or bulk permeability of a test region (such as a region in the vicinity of a borehole) including effects of fractures, fissures, anisotropy, and

Fig. 1. Applications illustrating the importance of concrete and grout permeability: (*a*) sewer pipes; (*b*) pressurized pipelines; (*c*) water storage structure; (*d*) gravity dams; (*e*) grouted fractures; and (*f*) concrete-encapsulated low-level radioactive waste.
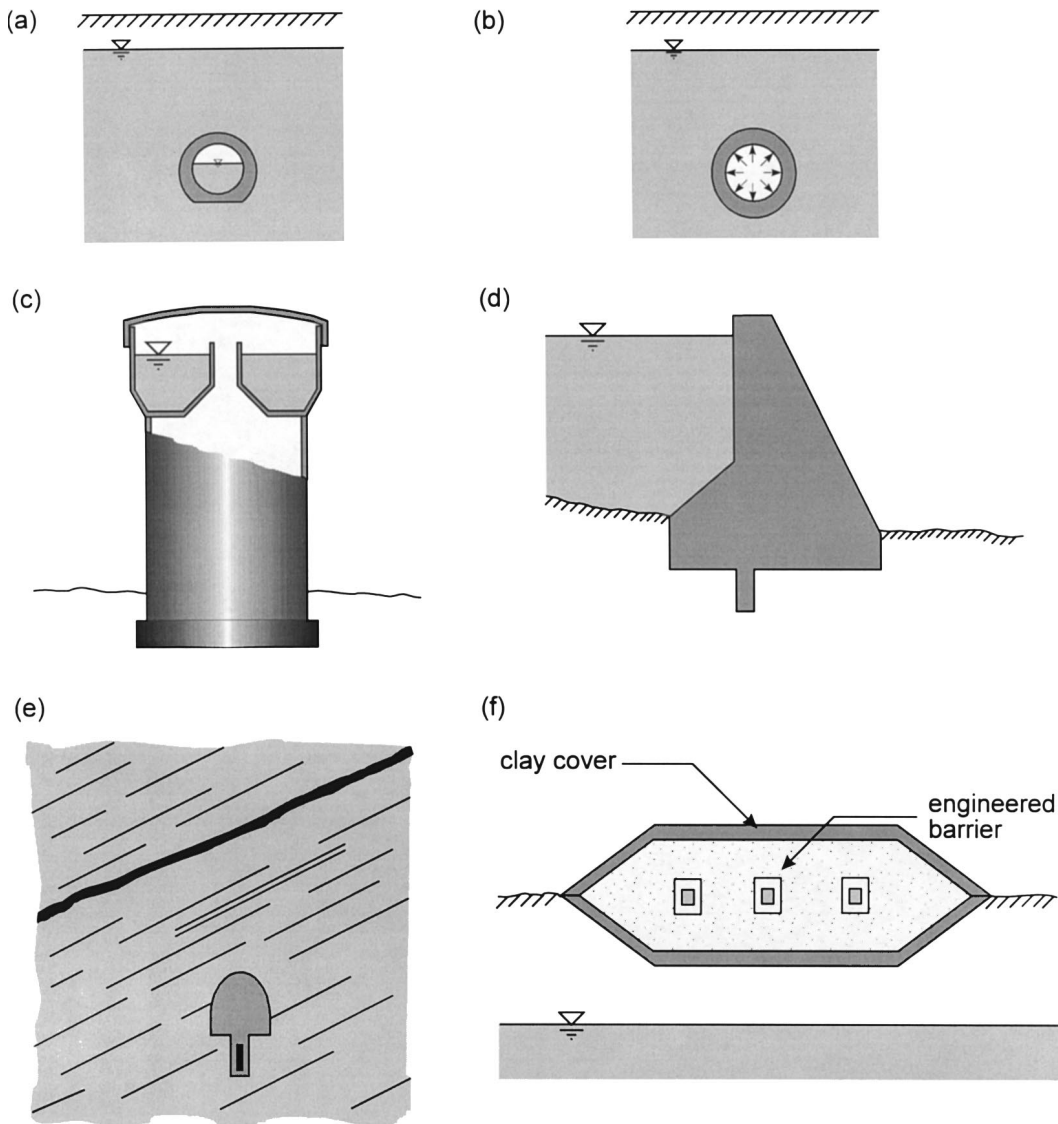
nonhomogeneity within that region. Laboratory testing techniques are carried out on small sized test specimens (e.g., 15 cm in diameter and 30 cm in length or smaller). The relatively small size of the test specimen usually ensures that the test material is in an intact state and that the chemical and pore structure of the material are not expected to vary significantly throughout the test specimen.

3.1. *In situ* permeability testing

The packer test is the most common method for measuring the in situ permeability of rock formations. In this method a test section of an exploratory borehole is isolated by internal sealing of the hole with an inflatable "packer." A single packer system uses a single inflatable section and seals between the base of the borehole and the inflatable packer. A double packer system seals a length of borehole between two inflatable packers. A known flow rate is injected into the isolated section of the borehole and the total head in the test section and in an observation well at a distance R from the test hole are recorded

once a steady state condition has been reached. The most commonly performed packer tests do not make use of an observation borehole. These simplified packer tests use an empirically derived coefficient, which depends on the ratio of hydraulic conductivities parallel and perpendicular to the borehole along with the injection rate and the total head in the test section, to evaluate the "average" permeability of the rock formation in the test section. The empirical coefficient chosen can also be based on a visual evaluation of the isotropy of the rock formation (Franklin and Dusseault 1989). Packer tests can also be used to perform pulse tests. In this technique, a section of a borehole to be tested and the connecting tubes are filled with water and then very rapidly pressurized and the pressure shut in. The pressure decay within the test section is recorded and the "transmissivity" of the test section is determined by using an appropriate theoretical development.

Borehole recharge tests or slug tests, although not very accurate, can be used to provide an estimate of the permeability. The elevation of the water table is measured in the borehole

and the water level is then lowered. The rise of water in the borehole over a period of time is recorded. Thus data can be used to estimate the average permeability of the material surrounding the borehole. Either exact or approximate mathematical solutions are used to calculate the permeability.

As is evident, in order to conduct an in situ type permeability test, it is essential to have access to a borehole. While such facilities are readily available for the in situ testing of geological materials, their use in the in situ permeability testing of concrete is uncommon and, due to the destructive nature of the test, they are largely unwarranted. The use of in situ permeability testing of concrete can, however, be considered feasible for large mass concrete structures such as dams and other water retaining structures.

3.2. Laboratory determination of permeability

The laboratory determination of permeability usually involves either the application of a constant pressure gradient across a sample and the measurement of the steady-state flow rate, or the application of a constant flow rate through the sample and the measurement of the corresponding equilibrium pressure. The constant pressure gradient test is by far the most common of the two techniques, but both techniques have their advantages.

The most common configuration for the steady state testing of permeability involves the one-dimensional testing of a specimen with rectilinear laminar flow. Typically, a constant pressure gradient is applied over the length of the sample and the flow rate of the fluid through the sample is measured. The main advantage of the steady state tests is its simplicity of analysis. In almost all cases, the permeability of the porous material can be calculated from a knowledge of the area over which the flow takes place, the hydraulic gradient, and the volume flow rate through the sample. The primary disadvantage of the steady state technique is that for materials with very low permeability, such as concrete or rock, long periods of testing are necessary to achieve a steady state flow condition (Poon et al. 1986; Banthia and Mindess 1989; Ahmed et al. 1991). Tests conducted by Powers et al. (1954) on approximately 25 mm diameter and 12 mm thick tapered cylindrical samples of cement pastes and rocks indicate that a duration of nearly 28 days is required to achieve steady state conditions. The second disadvantage of a steady state test is that the flow rates generated even under extremely large pressure gradients are extremely small (sometimes only fractions of a millilitre per hour). Accurate measurement of such low flow rates can be extremely difficult, owing to either instrument error or evaporation of the permeant during an experiment. A further limitation of a constant rate permeability test is the likelihood of secondary flow that could take place at the interface between the sample and the holder. In certain cases this leakage can be substantial and can be comparable to the flow rate through the sample. To minimize such leakage, pressures can be applied to the flexible sample holder; these stresses, however, can influence the flow characteristics through the sample. Some of the earliest versions of constant head permeability tests for rock cores were performed in triaxial cells. Daw (1971) described a permeameter constructed by modifying a commercially available Hoek–Franklin cell for triaxial testing of rock samples.

A transient one-dimensional flow technique for determining permeability was introduced by Brace et al. (1968). The tests were performed on cores of Westerly granite which were 1.61 cm long and 2.52 cm in diameter. The ends of the specimens were ground to form right cylinders. A specimen was positioned over the top of a hardened steel alloy plug which served as a downstream reservoir. A hollow piston, which is connected to the pressure supply, and a transducer positioned over the top of the sample. The hollow piston serves as the lid of the pressure cell and as the upstream reservoir. A 3 mm thick polyurethane rubber jacket which surrounds the sample, the alloy plug, and the hollow piston are held in place by wire clamps. The test specimen assembly is housed in a pressure cell (Fig. 2). The upstream and the downstream reservoirs are filled with water. The pressure cell is also filled with water and pressurized to a constant value. At the start of the test, the pressure in the upstream reservoir, P_U, is increased by 5%. The ensuing pressure decay in the upstream reservoir is recorded for a test period of 30 min.

Since the test specimen is within a closed system, the pressure in the downstream reservoir, P_D, increases as P_U decreases until an equilibrium pressure P_f is reached in both reservoirs. A plot of $(P_U - P_f)$ vs. time is made on a semi-log scale, and this result along with a simplified solution of the differential equation governing one-dimensional transient flow of a compressible fluid through a porous medium is used to evaluate the permeability K. In contrast to steady state tests, which require considerable time to perform and involve the measurement of extremely low flow rates, the transient tests can be performed relatively quickly and involve only low fluid volume movements through the porous medium; the influences of which are inferred through variations in a pressure field.

Techniques that measure parameters that can be related to permeability can be considered as "indirect" methods. An example of such an indirect technique is the use of a scanning electron microscope to observe the arrangement of particles and void configuration in thin sections of the material. The images can then be digitized by a computer, and the pore size and shape distributions can be used to create a theoretically representative model of the porous material including its permeability (Bear 1972; Scheidegger 1974; Schlueter et al. 1991; Dullien 1992).

4. Experimental methodology

From a review of the existing tests for the measurement of permeability characteristics of very low permeability materials, it is clear that a transient technique is the most desirable procedure. Furthermore, in order to avoid problems attributed to the Klinkenberg effect, it is necessary to use water as the permeating fluid. Although the principles of the "transient pulse" test are well established and the technique has been used by Brace et al. (1968) for rectilinear one-dimensional tests, in this paper a more versatile test procedure involving radial flow conditions will be proposed.

The test procedure proposed basically deals with the radial flow from the central cavity contained in a cylindrical sample of the porous medium. A nearly instantaneous pressure pulse is applied to the central cavity. The resulting pressure gradient causes radial flow and this results in the decay of the pressure within the cavity. The time dependence of the decay is a function of the permeability of the test specimen. A schematic view

Fig. 2. The confined sample arrangement used in transient pulse test (after Brace et al. 1968).
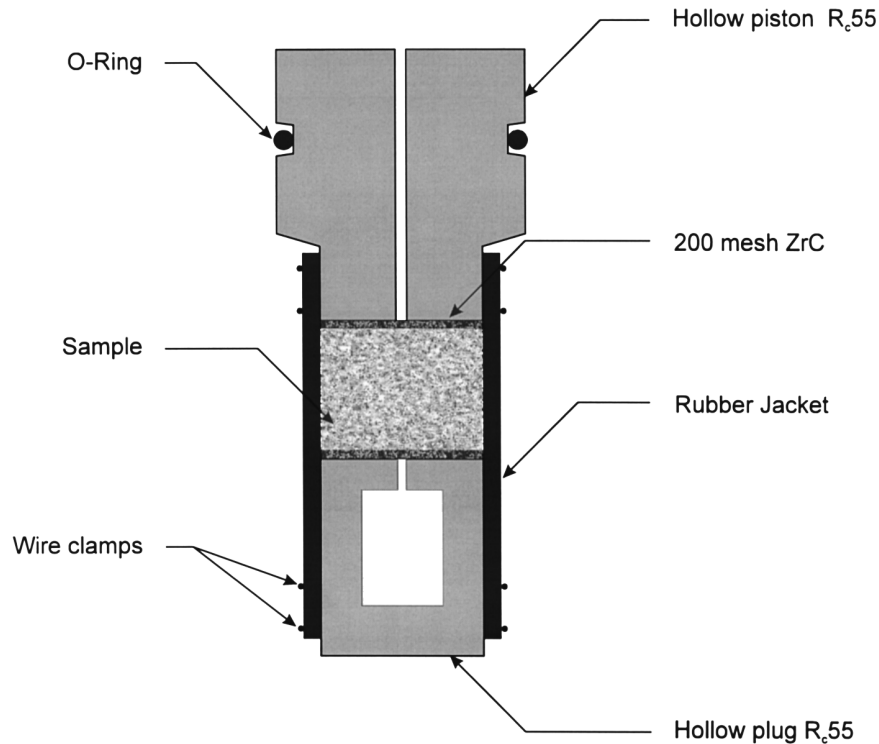
of the proposed test is shown in Figs. 3*a* and 3*b*. The experimental facility consists of three main components: the test specimen assembly, the fluid pressure supply, and the data acquisition system. The pressure supply and the data acquisition components were commercially available items. The test specimen assembly required a detailed examination of the factors affecting the test, and the resulting design makes the test a novel development. The test specimen assembly consists of three main components: the water chamber, the upper loading plate, and the reaction frame. All components of the assembly which come in direct contact with the permeating fluid and (or) the test material were fabricated from stainless steel to ensure long-term durability of the apparatus and resistance to reactions with either the permeating fluid and (or) the test material. The stainless steel water chamber has an inside diameter of 292 mm and a depth of 305 mm. The volumetric capacity of the chamber is 20.4 L. The size of the chamber is sufficient for testing specimens as large as 150 mm in diameter and 250 mm in height. The chamber is made sufficiently large to provide unrestricted work space during the positioning of the specimen. A flange at the base of the chamber wall seals against an O-ring in the base plate. The upper flange has an O-ring groove in it, which allows a lid to be sealed over the top of the water chamber in order to use it as a vacuum chamber.

The base of the water chamber is made of a stainless steel plate 400 mm × 400 mm × 12.7 mm, which has been machined smooth over the entire upper surface. An O-ring seated in the centre of the top surface of the plate is used to provide a seal between the plate and the test specimen. In order to measure the pressure in the central cavity of the test specimen, a transducer is positioned in the base plate. The upper loading plate serves both as a loading head against which the test speci-

men is sealed (using an O-ring seal) and as the manifold for the fluid pressure inlet to the cylindrical cavity and the bleeder port. It was designed to fit precisely at the upper surface of a 150 mm diameter test specimen, but can also be used with samples of smaller diameter. Stainless steel elbow fittings which have been welded into the sides of the plate provide fluid access to the sealed cavity in the test specimen. The free ends of the elbows have Swagelok tube connector fittings. One elbow is connected to a Nupro plug valve which seals in the fluid pressure, while the second serves as a bleeder valve. A depression was machined in the centre of the upper plate to accommodate a steel ball bearing through which the axial load is applied to the sample. This arrangement ensures that the axial load is applied through the centre of the test cylinder. The reaction frame consists of a rigid base, two threaded rods, and a cross head. Access for the leads from the pressure transducer is provided through the base of the loading frame. A load cell which is attached to the underside of the cross head of the testing frame measures the load as the beam is tightened down.

The data acquisition system consisted of commercially available components. The fluid pressure within the cavity of the test specimen is measured using a DCT Instruments PZA 100AC series port style pressure transducer. The transducer is rated for an operating pressure of 690 kPa and has an error of 0.50% of full scale due to nonlinearity and hysteresis. The temperature of the water was monitored via a type K thermocouple. The load cell (Interface model 1210 AF with a rated capacity of 44.5 kN) enables all tests to be carried out at the same axial stress conditions. The load cell has an error due to nonlinearity of ±0.05% at the full-scale reading. The pressure transducer, the load cell, and the thermocouple readings are collected and stored on disk via a computerized data acquisition system. The system consists of a commercially available

Fig 3*a*. A schematic diagram of the proposed test.
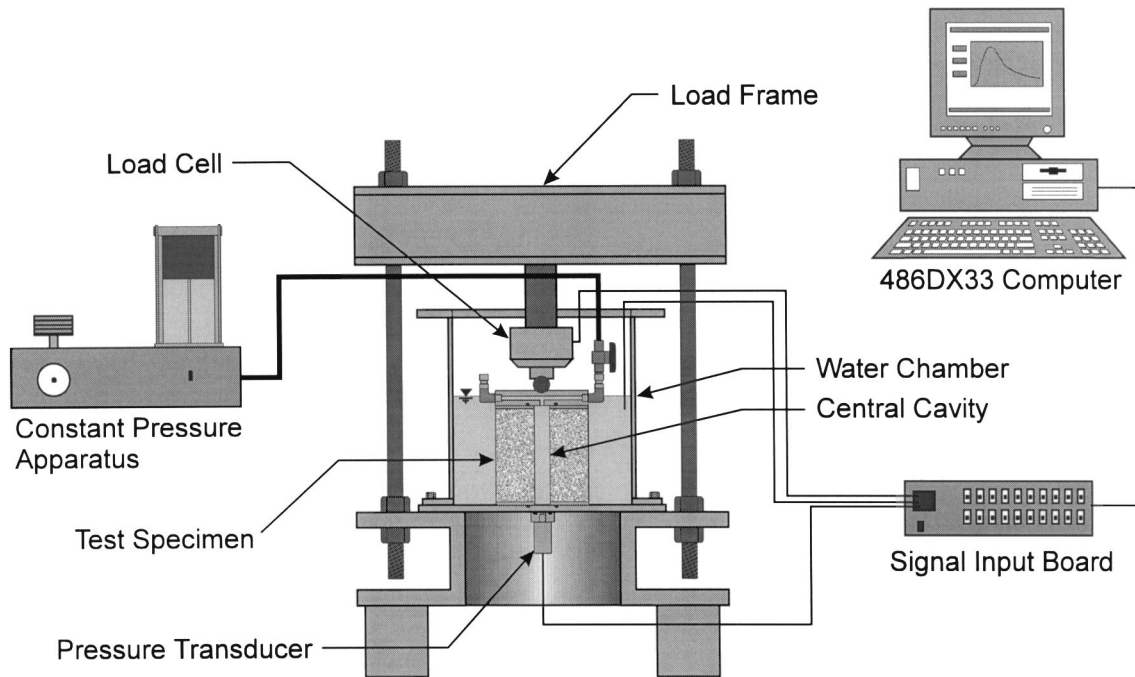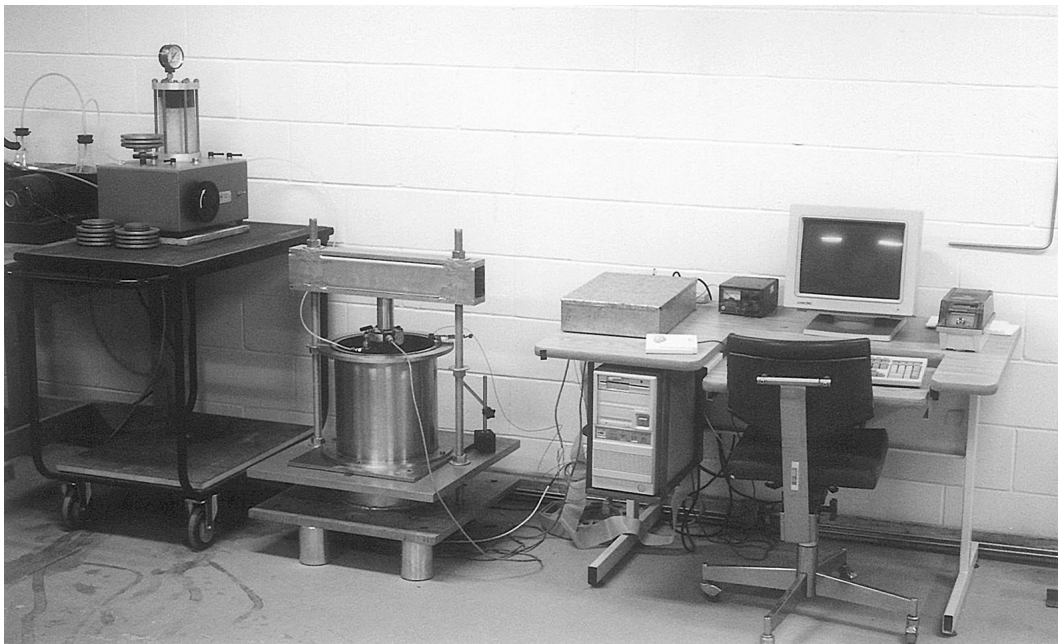

Fig. 3*b*. A general view of the experimental setup for conducting transient pulse tests.

package from National Instruments Corporation and includes an AMUX-64T analog multiplexer with temperature sensor and an AT-MIO-16F-5 data acquisition board which is incorporated in a 486 DX 33PC computer installed with the Lab-Windows software package. The software package allows the data acquisition program to be custom designed. A DC power supply is used to provide the excitation voltage to both the load cell and the pressure transducer.

In this experimental program, tap water was used as the permeating fluid. The pressure supply to the cavity was provided

by a constant pressure apparatus designed for use with triaxial soils testing equipment. An EL 27-432 series constant pressure supply can maintain a constant pressure between 100 and 3500 kPa. In order to provide a complete seal between the test specimen and the upper and lower plates, it is necessary to ensure that the end surfaces are flat and parallel. The desired end conditions were achieved by grinding the ends of the test specimen in a concrete cylinder grinder and attaching the machined stainless steel end plates with an adhesive resin (Bondo marine resin). The resin serves to seal the pores at the exposed

end surfaces of the specimen and to attach the end plates. The principal assumption in the experimental methodology of the proposed permeability test is that the pressure decay in the central cavity is entirely due to the outward radial flow of the pressurized fluid through the porous test specimen. Tests were performed to confirm the validity of this assumption. An impermeable test specimen was fabricated from a solid aluminum cylinder. The end faces of the cylinder (113 mm outside diameter, 25.4 mm inside diameter, and 150.8 mm in height) were machined smooth and parallel. Tests were carried out with the solid cylinder and modifications to the seals and fittings were made until a negligible loss of pressure could be observed over a period of time well in excess of the time required to conduct permeability tests on samples made from cement grout. The details of the confirmatory experiments are given by Carnaffan (1994).

5. Sample preparation and the experimental procedure

In this phase of the research program, the experimental modelling was restricted to fabricated cylindrical samples of grout. The choice of the grout as a test material is dictated by three considerations. First, the primary objective of the test is to determine the permeability of fine grained materials such as grouts which are proposed as sealing materials in geoenvironmental applications. Second, the dimensions of the test specimen would not lend itself for use with concrete specimens where the aggregate sizes would be comparable to the internal radius of the cylinder. Furthermore, the creation of a cavity by drilling, no matter how carefully this may be done, will induce dynamic stresses, which can cause debonding at the aggregate matrix interface and which in turn can lead to an erroneous interpretation of the test results. This can be alleviated to a certain extent, either by casting concrete cylinders with a former for creation of the internal cavity or by substantially increasing the dimensions of the test specimen. These modifications are, however, relegated to future work. Third, the cement grout offers the possibility of conducting tests on a material where the variability in the material properties can be kept to a minimum. This aspect is important particularly at the early stages of the development of a novel testing method where any radical variations can be interpreted as errors in the testing methodology, as opposed to material variability.

For the purposes of the experimentation, ten grout cylinders measuring 150 mm in diameter and 300 mm in length were fabricated. The Sika 212 grout mixture was mixed in a portable drum mixer as per instructions of the supplier. The workability of the mix was such that any air voids could be readily removed by tapping of the sides of the cylinders. Six cylinders measuring 75 mm in diameter and 150 mm in length were also fabricated. The cylinders were allowed to harden for a period of 24 h, after which they were stripped from their moulds and left to cure in a curing room for 28 d. After the curing period, 10 mm of the top end of each cylinder was cut off using a masonry saw. All the test cylinders were cored out with a 25 mm nominal diameter diamond tooth coring bit. The cores were subsequently used to measure the void content of the grout. Both ends of the cylinder were cut with the masonry saw so that the cylinders were approximately 235 mm in length. The ends of the cylinders were ground smooth and parallel

using a concrete cylinder grinder. The final external dimensions of the test cylinders were 225 mm in length and 152 mm in diameter with a central cavity of diameter 26 mm. Stainless steel plates were then bonded to the finished cylinders using the epoxy adhesion procedure described by Carnaffan (1994).

The experimental procedure which was followed in performing the transient pulse tests is summarized for completeness. (Further details are given in Carnaffan (1994).)

(a) The test specimen was vacuum saturated with water. The vacuum pump was connected to a timer switch which operated the pump in an on–off mode every 30 min. This on–off cycle was operated for 96 h.

(b) The sample was transferred to the test chamber, which was already filled with water, and positioned in the centre so that the pressure transducer at the base plate was exposed to the water in the central cavity of the test specimen. The upper plate was positioned on the sample and all the ports in the plate were exposed to water. The water level in the chamber was kept at approximately 25 mm below the upper level of the chamber. In this condition the sample and the connecting couplings are subjected to vacuum for a period of 4 h.

(c) All connections to the pressurizing system were made in a submerged condition. This was intended to eliminate any entrapped air in the pressurized system.

(d) The water level in the exterior region was lowered (by siphoning) to the mid-section of the upper plate.

(e) The sensors were connected to the data acquisition system and the computer system activated.

(f) The cross head was positioned so that the load cell was in contact with the spherical seating. The cross head was tightened until an axial load of 5000 N was registered by the load cell. The test sample was left in the loaded condition until all excess pore water pressures induced during the application of the 5000 N load was dissipated.

(g) The constant pressure apparatus was connected to the upper plate and a nominal pressure (100 kPa) was applied to remove any air from the system.

(h) The fluid in the internal cavity was subjected to a pressure of 600 kPa within a 10 s interval.

(i) Upon attainment of the prescribed internal pressure, the valve connection to the pressure supply was closed and the data acquisition sequence commenced. The first set of readings of the axial load, the pressure within the cavity, and the temperature of the system were taken after 30 s and subsequent readings were taken at every 300 s.

(j) The data acquisition was terminated after 3 h. At this point, the bleeder valve was opened and the test sample was left for 24 h to allow dissipation of any excess pore pressures.

(k) This test procedure was repeated from step (g) onwards to derive three separate sets of data for each sample.

The proposed test procedure provided several advantages over the transient pulse test proposed by Brace et al. (1968). First, the equipment and the test procedure were much simpler, since no circumferential confining pressure had to be applied to the test specimen. Furthermore, there was no requirement for the provision of a high pressure chamber or a rubber sealing sleeve. Second, the axial loads applied to the sample were nominal. The methodology proposed by Brace et al. (1968) required a confining pressure of at least 1.2 times the applied pressure in order to minimize flow at the boundary. Rough textured core samples sometimes required a confining pressure

as high as twice the fluid pressure required to initiate flow. The proposed test required only a nominal axial load to seal the pressurized internal cavity region. Finally, the geometry of the test allowed for the monitoring of the pressure decay within the internal cavity with considerable accuracy. Also, the radial symmetry of the problem was amenable to straightforward theoretical modelling.

6. Theoretical modelling

We first consider the problem of the transient radial flow from a pressurized borehole of radius a which is located in a saturated porous medium of infinite extent. We assume that the flow of water in the porous medium is governed by Darcy's Law. The pore fluid is assumed to be compressible. We also assume that the porosity of the medium is influenced by only the bulk compressibility of the medium. The volume of solids composing the porous medium is assumed to be incompressible in comparison with the pore fluid and the porous skeletal fabric. By considering equations of continuity and Darcy's Law, it can be shown (Freeze and Cherry 1979; Hsieh et al. 1981; Fetter 1988; Barenblatt et al. 1990) that the differential equation governing the transient variation of head, h, (dimension L) in the region due to pressurization is given by

[1] $\quad \nabla^2 h = \dfrac{S}{T_R} \dfrac{\partial h}{\partial t}$

where

[2] $\quad \nabla^2 = \dfrac{\partial^2}{\partial r^2} + \dfrac{1}{r} \dfrac{\partial}{\partial r}$

is Laplace's operator referred to the radially symmetric coordinate system. In [1], S (non-dimensional) is the storage coefficient of the tested interval ℓ (dimension L) defined by

[3] $\quad S = \ell \gamma_w \left[n C_w + C_{eff} \right]$

where γ_w is the unit weight of water (dimension M/L^2T^2); C_w is the compressibility of water (dimension LT^2/M); C_{eff} is the compressibility of the porous skeleton (dimension LT^2/M); n is the porosity (non-dimensional); T_R is the transmissivity of the tested interval (dimension L^2/T) (Haimson and Doe 1983) which is related to k, the hydraulic conductivity of the porous medium (dimension L/T), by the relationship

[4] $\quad T_R = k\ell = \dfrac{K\ell\gamma_w}{\eta}$

where K is the permeability of the porous medium (dimension L^2); and η is the kinematic viscosity of water (dimension M/LT). Equation [1] is an approximation to the more generalized situation involving full coupling between the deformations of the pore fluid and the deformations of the porous skeleton (Biot 1941; McNamee and Gibson 1960; Rice and Cleary 1976; Selvadurai and Yue 1994; Selvadurai and Nguyen 1995; Selvadurai 1996). Although the porous skeleton is assumed to be non-deformable, account is made for a bulk volume change of the porous skeleton. An alternative to this approach is to assume that the porous skeleton is perfectly rigid; in which case C_{eff} is set equal to zero.

Considering the experimental arrangement, we examine the problem of radial flow from the pressurized central cavity for

which the governing initial and boundary conditions are as follows:

[5] $\quad h(r, 0) = 0$

[6] $\quad h(\infty, t) = 0$

[7] $\quad h(a, t) = H(t)$

[8] $\quad H(0) = H_0$

[9] $\quad 2\pi a T_R \left(\dfrac{\partial h}{\partial r} \right)_{r=a} = V_w C_w \gamma_w \dfrac{\partial H}{\partial t}$

The boundary condition [5] implies that at the start of the experiment the head distribution in the sample is uniform and defined to be zero. The boundary condition [6] implies that the outer boundary of the sample is remotely located from the inner boundary and that the head at that boundary is maintained at zero, at all times.

The boundary conditions [7] and [8] indicate that the head within the cavity is a time-dependent variable and has a constant value at $t = 0$. The boundary condition [9] states that the rate at which water flows from the cavity into the cylinder, as expressed by Darcy's Law applied to the inner cavity, is equal to the rate at which the water stored within the pressurized cavity expands as the pressure within the system declines. In [9], V_w refers to the volume of water (dimension L^3) within the pressurized section of the system, which could include the volume of water in the leads of the apparatus. It must be noted that the boundary condition [6] is an approximation, the accuracy of which needs to be verified particularly in relation to the finite outer dimension of the test cylinder. This assumption, however, considerably simplifies the mathematical analysis of the differential equation [1] which governs the transient flow in the porous medium.

The solution of [1] subject to the initial conditions and boundary conditions, [5] – [9], has been studied in detail in connection with both the non-steady ground water flow and the analogous problem in heat conduction (Jacob 1940, 1947; Carslaw and Jaeger 1959; Cooper et al. 1967; Papadopulos et al. 1973; Bredehoeft and Papadopulos 1980; Hodgkinson and Barker 1985; Rutquist 1995). Avoiding details of these analyses we record here the salient result that pertains to the decay of head within the pressurized cavity, which can be expressed in the form

[10] $\quad \dfrac{H(t)}{H_0} = F(\alpha, \beta)$

where

[11] $\quad \alpha = \dfrac{\pi a^2 S}{V_w C_w \gamma_w}; \qquad \beta = \dfrac{\pi T_R t}{V_w C_w \gamma_w}$

Also, the function $F(\alpha, \beta)$ can be expressed in the integral form:

[12] $\quad F(\alpha, \beta) = \dfrac{8\alpha}{\pi^2} \displaystyle\int_0^\infty \dfrac{\exp(-\beta u^2/\alpha)}{u f(u, \alpha)} \, du$

where

[13] $\quad f(u, \alpha) = \left[u J_0(u) - 2\alpha J_1(u) \right]^2 + \left[u Y_0(u) - 2\alpha Y_1(u) \right]^2$

Also, $J_0(u)$ and $J_1(u)$ are, respectively, zero-order and

first-order Bessel functions of the first kind; and $Y_0(u)$ and $Y_1(u)$ are, respectively, zero-order and first-order Bessel functions of the second kind (Watson 1944). Tabulated values for $F(\alpha, \beta)$ are given in Cooper et al. (1967) and Papadopulos et al. (1973) and will not be repeated here. Also, Bredehoeft and Papadopulos (1980) have presented a useful approximation for the integral [12] in the form:

[14] $F(\alpha, \beta) \simeq e^{4\alpha\beta} \, \text{erfc}(2\sqrt{\alpha\beta}\,)$

where erfc is the complimentary error function, the tabulated values of which are given in Abramowitz and Stegun (1964). Bredehoeft and Papadopulos (1980) have shown that for $\alpha > 10$, the results [12] and [14] are virtually identical. For values of α less than 0.1, these authors have provided numerical values of $F(\alpha, \beta)$ which can be used for purposes of evaluating test data. They also conclude that an error of two orders of magnitude in the estimation of α would result only in an error of less than 30% in the determined value of T_R.

In the preceding developments we have explicitly assumed the boundary condition [6], which is applicable to a medium of infinite extent rather than an annular region with a finite outer radius $r = b$. It is therefore necessary to prove the limits of applicability of the results [12] and [14] to an annular region bounded by $r \,\varepsilon\, (a, b)$. The applicability of the simplified result [10] to the annular porous region used in the experimental configuration is further verified in Appendix A.

7. Experimental results

The theoretical developments outlined in the previous section require the use of constitutive parameters such as the compressibility of the unsaturated grout, C_{eff}, and physical parameters such as the porosity, n, of the grout. In order to evaluate the compressibility of the porous grout skeleton, it is necessary to determine the elastic modulus, E, and Poisson's ratio, ν, of the grout material. These material properties can be accurately determined by recourse the test procedures outlined in the relevant ASTM standards.

The porosity of the grout was determined by performing void ratio tests in accordance with ASTM 642-82. The cylindrical samples recovered from the coring of the test cylinders were used for this purpose. The porosity, n, is related to the void ratio, e, through the relationship:

[15] $n = \dfrac{e}{1 + e}$

Three grout cylinders measuring 75 mm in diameter and 150 mm in length were used for the determination of the elastic modulus and Poisson's ratio. Two strain gauges were mounted at mid-height of each cylinder. The strain gauges of gauge length 8 mm (Showa model N11-FA-8-120-11) were mounted at mid-height of each cylinder. One strain gauge was oriented in the longitudinal direction and the other in the circumferential direction. The ends of the cylinders were capped to provide parallel ends. The cylinders were tested in compression according to ASTM C39. The loading rate was 1.3 mm/min. The elastic modulus and Poisson's ratio were determined from the stress–strain response. The bulk compressibility of the grout material was calculated using the relationship:

[16] $C_{\text{eff}} = \dfrac{3(1 - 2\nu)}{E}$

A summary of the average values of the elasticity and physical properties of the cement grout, which can be used in the theoretical computations, is as follows:

Elastic modulus, $E = 19.231$ GPa ($\pm$124 MPa)

Poisson's ratio, $\nu = 0.21$ ($\pm$0.01)

Bulk compressibility, $C_{\text{eff}} = 90.48 \times 10^{-9}$ m^2/kN

Void ratio, $e = 0.229$ ($\pm$0.006)

Porosity, $n = 0.186$

In total, seven cylinders of the cement grout were used in preliminary tests for the purposes of evaluating the effectiveness of the seals employed in the test facility. The three cylinders used in the final experiments are designated samples 1, 2, and 3. Three consecutive tests were carried out on each of the test specimens. The three tests are designated A, B, and C. All tests were carried out in accordance with the procedures described in the previous section, at an initial pressure of 600 kPa. In all tests, ordinary tap water at room temperature was used as the permeating fluid. The physical and mechanical properties of water required in the theoretical calculations were taken from published values (White 1986). The parameters applicable to the general temperature and pressure ranges of the tests (room temperature of 20°C to 22°C and atmospheric pressure) are as follows:
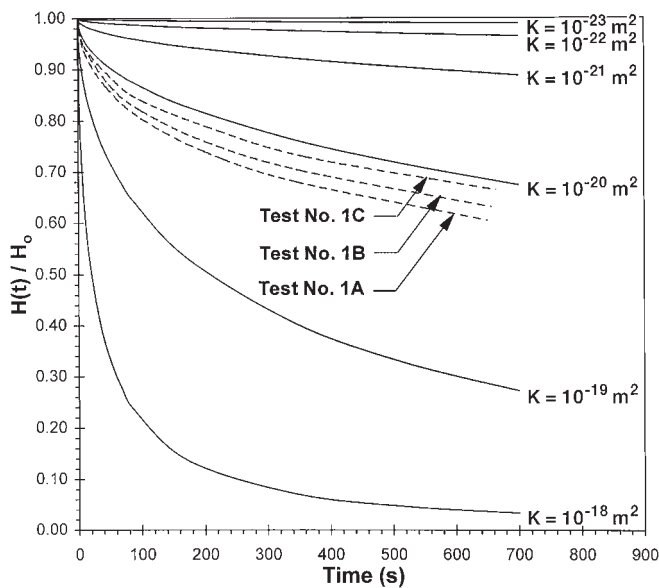
Unit weight, $\gamma_w = 9.81$ kN/m^3

Viscosity, $\mu = 10^{-6}$ kN·s/m^2

Compressibility, $C_w = 454.10 \times 10^{-9}$ m^2/kN

The experimental results have been plotted in the form of a non-dimensional pressure $P(t)/P_0$ vs. time. The theoretical estimates for the pressure decay in the cylindrical cavity were generated by the result [10] in conjunction with [12]. The value of α for this series of tests was found to be less than 10 ($\alpha = 0.34$). Consequently, [12] can also be evaluated by using the tables provided by Bredehoeft and Papadopulos (1980).

Figure 4 illustrates the experimental results for the pressure decay in the cylindrical cavity (shown in broken lines) derived from the three tests conducted on the same sample of cement grout. Figure 4 also illustrates the theoretical estimates for the pressure decay determined for several choices of K ranging from 10^{-18} to 10^{-23} m^2. This graphical representation allows us to narrow down a "range of interest" for the value of K, which can be used to match closely the pressure decay results derived from sample 1 with the theoretical estimates. Figures 5–7 illustrate comparisons between the experimental results and the theoretical estimates for a range of values of K obtained for the three successive tests conducted on sample 1 with tests designated 1A, 1B, and 1C. Similarly, Figs. 8 and 9 illustrate the preliminary comparisons between the experimental results and the theoretical estimates obtained for the tests conducted on samples 2 and 3. Again, individual evaluations have been conducted to narrow down the range of values of K. In these comparisons, the theoretical predictions which closely match the experimental observations yield the respective value of K. Admittedly, it is possible to strive for a perfect match between

Fig. 4. Experimental results for pressure decay curves derived from three tests conducted on sample 1.

Fig. 5. Experimental results from test 1A and comparison with theoretical decay curves corresponding to $K \varepsilon$ (10^{-19}, 10^{-21}) m^2.


the experimental results and theoretical predictions using either further refinement in the range of values of K or by using statistical techniques (e.g., a least square fit between the experimental results and theoretical estimates). Such a degree of refinement is perhaps unwarranted in view of the approximations invoked in the theoretical developments. For this reason, the correlation is established by interpolating the value of K for the experimental results from the values of K corresponding to the theoretical predictions which "bound" the experimental result. The average permeability of each specimen was calculated using the results of the three tests, A, B, and C. The summary of the results is shown in Table 1. It can also be noted that the results derived from these tests are in the same range as the results published by Bamforth (1987) and Banthia and Mindess (1989) for "steady state" tests conducted on several different mixes of hardened cement paste. The range of permeabilities obtained by these researchers was between 10^{-18} and 10^{-21} m^2. The permeability of the grout measured using the "transient" procedure ranged from 10^{-20} to 10^{-21} m^2.

8. Concluding remarks

This paper documents a novel laboratory experimental procedure which can be performed to determine the permeability characteristics of low permeability materials such as cement grouts, concrete, and rocks. The transient pressure pulse technique can be performed relatively quickly in comparison with many steady state test procedures advocated in the literature. The saturation of the sample is an important consideration in the determination of permeability characteristics of porous materials with relatively low permeability. It was found that approximately 4 days were required to saturate the test samples. This duration could be reduced by using either smaller test samples or samples with a relatively larger inner to outer diameter ratio. The transient tests were conducted for 3 h; however, only the first 600 s of data were required to determine the permeability of the material. This estimate of the time for a test
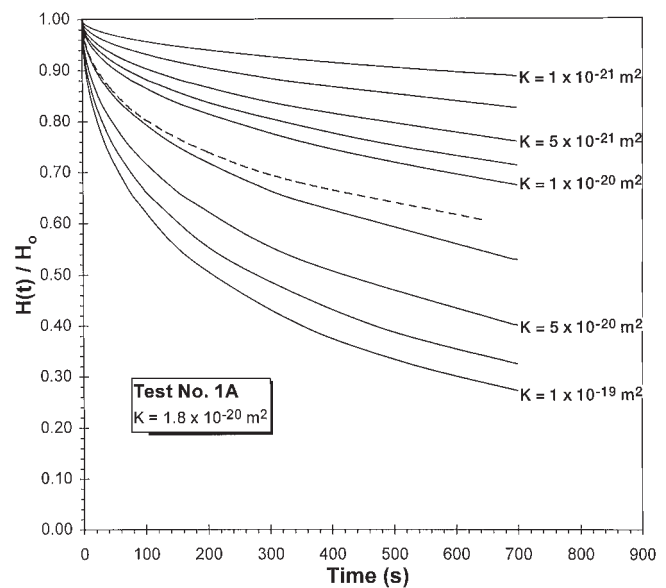
cannot be regarded as universally applicable. It is likely that data for longer periods of time would be required to identify the permeability of materials with permeabilities lower than 10^{-21} m^2. This is due to the fact that, for permeabilities beyond this value, the pressure decay in the central cavity is so small that the theoretical estimates for the decay curves would be much too closely spaced for an accurate evaluation of the permeability by matching theoretical and experimental estimates. The transient technique can be applied to determine the permeability of materials with permeabilities greater than 10^{-17} m^2, provided the pressure decay within the cavity can be scanned relatively rapidly by the data acquisition system. Alternatively, the experimental configuration can be easily adapted to conduct a steady state test involving a constant flow rate.

The values of permeability of the grout obtained from the experimental results and the associated theoretical models are comparable with the results for permeability of cement paste available in the literature. Admittedly, a direct comparison of the sets of data is unwarranted in view of the possible differences between the two materials. A consistent observation in these tests is the slight reduction in the permeability of the material for each subsequent test conducted on the sample. It is difficult to pin point any specific reason for this phenomenon. Possible influences could include the following: the complete saturation of the cement grout leading to a hydration of the cement and a subsequent reduction in the pore space; the elimination of the Klinkenberg effect due to the progressive increase in the saturation of the pore space; chemical reactions between the water and the cement grout leading to the precipitation of leached material in the pore space, resulting in a reduction in the permeability. (Similar effects have been observed by Vaughn (1987) in the permeability testing of heated granite.) This latter effect is most likely to be the cause, since a hard textured residue (most likely, calcium silicate) was observed on the outside of the test cylinders at the termination of the tests. In any event the trends in the slight reductions are consistent and within the range of accuracy both desirable and

Fig. 6. Experimental results from test 1B and comparison with theoretical decay curves corresponding to $K \varepsilon$ (10^{-19}, 10^{-21}) m^2.
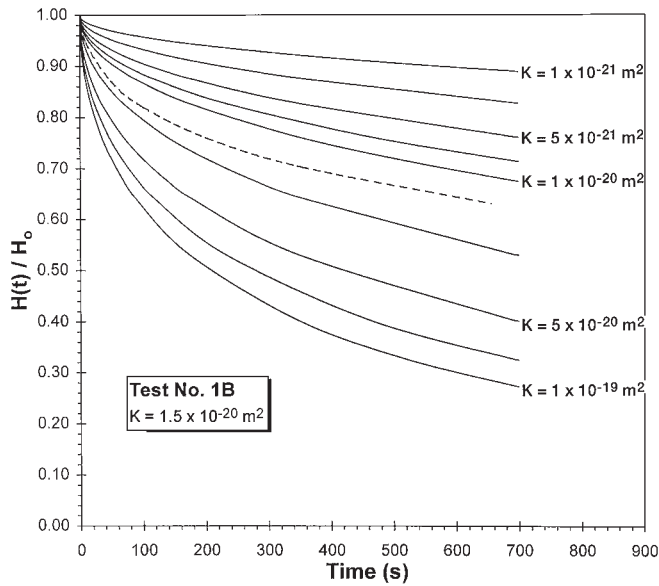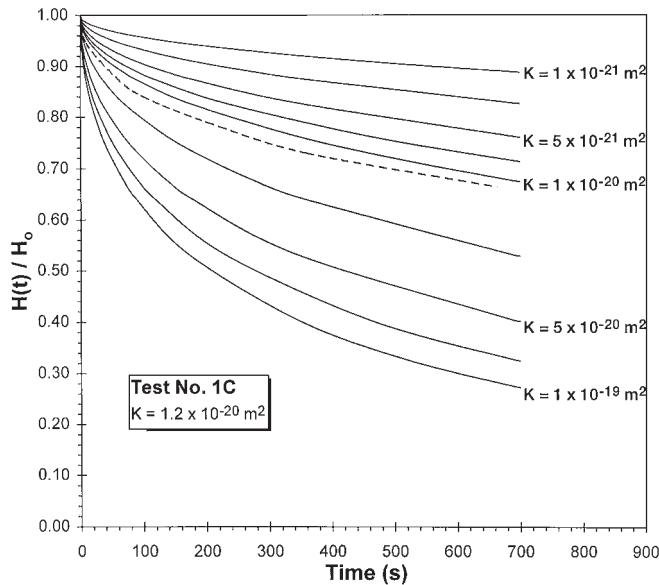

Fig. 8. Experimental results for pressure decay curves derived from three tests conducted on sample 2.

Fig. 7. Experimental results from test 1C and comparison with theoretical decay curves corresponding to $K \varepsilon$ (10^{-19}, 10^{-21}) m^2.
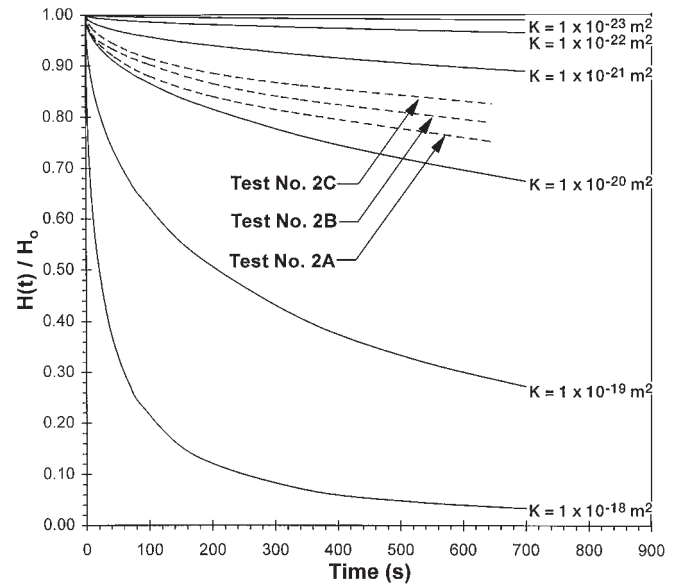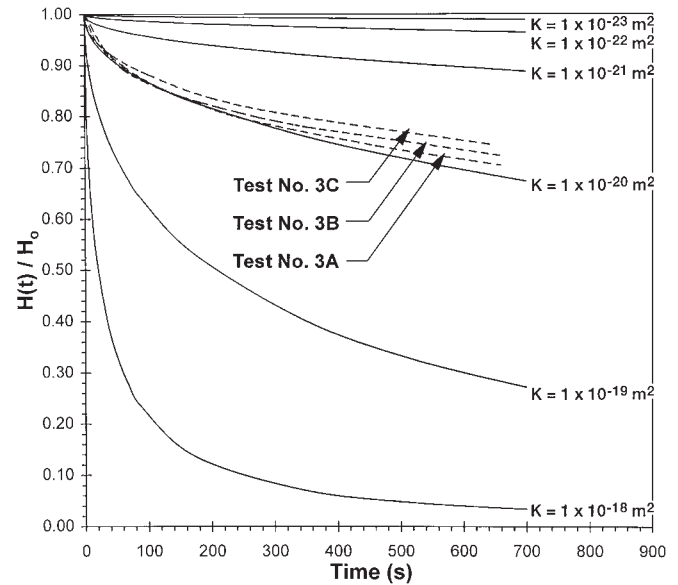

Fig. 9. Experimental results for pressure decay curves derived from three tests conducted on sample 3.

realistic for the evaluation of the permeability characteristics of the cement grout.

The primary advantage of the test is the ability to initiate a radial flow condition where the internal cavity can be sealed at the plane ends of the specimen to create the pressurized cavity. This method of testing has advantages over the one-dimensional procedure described in the literature, where the jacketed specimens need to be subjected to a separate confining pressure. In the preliminary phases of this research program, attention has been restricted to the determination of the permeability of a cementitious material such as grout. The experimental and theoretical concepts can be easily extended to include concrete and granite cylinders containing flat fractures and fractured concrete and granite specimens whose fractures are sealed with materials such as microfine grouts, epoxy, and other sealants. These studies will be reported in future publications.

Acknowledgements

Table 1. Permeability of cement grout — summary of results derived from pulse tests.

Sample	Test	Permeability (m²)	Average permeability (m²)
1	A	1.8×10^{20}	1.5×10^{-20}
	B	1.5×10^{-20}	
	C	1.2×10^{-20}	
2	A	6.0×10^{-21}	4.3×10^{-21}
	B	4.0×10^{-21}	
	C	2.8×10^{-21}	
3	A	8.5×10^{-21}	7.4×10^{-21}
	B	7.5×10^{-21}	
	C	6.3×10^{-21}	

Note: Average permeability = 8.9×10^{-21} m².

reviewers and the Associate Editor for their constructive comments.

References

Abramowitz, M., and Stegun, I.A. 1964. Handbook of mathematical functions. National Bureau of Standards, Applied Mathematics Series 55, U.S. Government Printing Office, Washington, D.C.

Ahmed, U., Crary, S.F., and Coates, G.R. 1991. Permeability estimation: the various sources and their interrelationships. Journal of Petroleum Technology, **43**(5): 578–587.

Bamforth, P.B. 1987. The relationship between permeability coefficients for concrete obtained using liquid and gas. Magazine of Concrete Research, **39**(138): 3–11.

Banthia, N., and Mindess, S. 1989. Water permeability of cement paste. Cement and Concrete Research, **19**: 727–736.

Barenblatt, E.I., Entov, V.M., and Ryzhik, V.M. 1990. Theory of fluid flow through natural rocks. Kluwer Academic Publishers, Dordrecht, The Netherlands.

Bear, J. 1972. Dynamics of fluids in porous media. American Elsevier, New York.

Bernaix, J. 1966. New laboratory methods of studying the mechanical properties of rocks. International Journal of Rock Mechanics and Mining Sciences, **6**: 43–89.

Biot, M.A. 1941. General theory of three-dimensional consolidation. Journal of Applied Physics, **12**: 155–164.

Brace, W.F., Walsh, J.B., and Frangos, W.T. 1968. Permeability of granite under high pressure. Journal of Geophysical Research, **73**(6): 2225–2236.

Bredehoeft, J.D., and Papadopulos, I.S. 1980. A method for determining the hydraulic properties of tight formations. Water Resources Research, **15**(1): 233–238.

Carnaffan, P. 1994. An experimental technique for determining the permeability of rock, concrete and cement grout. M.Eng. thesis, Department of Civil and Environmental Engineering, Carleton University, Ottawa, Ont.

Carslaw, H.S., and Jaeger, J.C. 1959. Conduction of heat in solids. Oxford University Press, Oxford, United Kingdom.

Cooper, H.H., Bredehoeft, J.D., and Papadopulos, I.S. 1967. Response of a finite-diameter well to an instantaneous charge of water. Water Resources Research, **3**(1): 263–269.

Corey, A.T. 1990. Mechanics of immiscible fluids in porous media. Water Resources Publishing, Littleton, Co.

Daw, G.P. 1971. A modified Hoek–Franklin triaxial cell for rock permeability measurements. Geotechnique, **21**(1): 89–91.

Dhir, R.K., and Byars, E.A. 1993. PFA concrete: permeation properties of cover to steel reinforcement. Cement and Concrete Research, **23**: 554–566.

Dixon, R.S., and Rosinger, E.L.J. 1984. The Canadian nuclear fuel waste management program: 1983 annual report. Atomic Energy of Canada Limited, Pinawa, Man., Report AECL-7811.

Dullien, F.A.L. 1992. Porous media: fluid transport and pore structure. Academic Press, New York.

Fetter, C.W. 1988. Applied hydrogeology. Merrill Publishing Co., Columbus, Ohio.

Franklin, J.A., and Dusseault, M.B. 1989. Rock engineering. McGraw-Hill Inc., New York.

Freeze, R.A., and Cherry, J.A. 1979. Groundwater. Prentice-Hall, Englewood Cliffs, N.J.

Gray, M.N. 1993. OECD/NEA international stripa project. Overview Volume III. Engineered Barriers, SKB, Stockholm, Sweden.

Haimson, B.C., and Doe, T.W. 1983. State of stress, permeability and fractures in the Precambrian Granite of northern Illinois. Journal of Geophysical Research, **88**: 7355–7371.

Heystee, R., and Roegiers, J.C. 1980. The effect of stress on the primary permeability of rock cores — a facet of hydraulic fracturing. Canadian Geotechnical Journal, **18**: 195–204.

Hodgkinson, D., and Barker, J. 1985. Specification of a test problem for HYDROCOIN level 1, case 1: transient flow from a borehole in a fractured permeable medium. Atomic Energy Authority, Harwell, United Kingdom, Report AERE, R11574.

Hsieh, P.A., Tracy, J.V., Neuzil, C.E., Bredehoeft, J.D., and Silliman, S.E. 1981. A transient laboratory method for determining the hydraulic properties of 'tight' rocks — I. Theory. International Journal of Rock Mechanics, Mining Sciences and Geomechanics Abstracts, **18**: 245–252.

Jacob, C.E. 1940. On the flow of water in an elastic artesian aquifer. Transactions of the American Geophysical Union, **21**: 574–586.

Jacob, C.E. 1947. Drawdown test to determine effective radius of artesian well. Transactions of the American Society of Civil Engineers, **112**: 1047–1064.

Johnson, L.H., Tait, J.C., Shoesmith, D.W., Crosthwaite, J.L., and Gray, M.N. 1994. The disposal of Canada's nuclear fuel waste: engineered barriers alternatives. Whiteshell Laboratories, Atomic Energy of Canada Limited, Pinawa, Man., Research Report, AECL-10718: COG 93-8,

Kay, T. 1992. Assessment and renovation of concrete structures. Longman Scientific and Technical, John Wiley & Sons, Inc., New York.

Knutson, C.F., and Bohor, B.F. 1963. Reservoir rock behaviour under moderate confining pressure. Proceedings, Fifth Symposium on Rock Mechanics, University of Minnesota, Minn., MacMillan, New York, pp. 627–659.

Kranz, R.L., Frankel, A.D., Engelder, T., and Scholz, C.H. 1979. The permeability of whole and jointed barre granite. International Journal of Rock Mechanics, Mining Sciences and Geomechanics Abstracts, **16**: 225–234.

Laughton, A.S., Roberts, L.E.J., Wilkinson, D., and Gray, D.A. (*Editors*). 1986. The disposal of long-lived and highly radioactive wastes. Proceedings of the Royal Society, Discussion Meeting, Royal Society, London, United Kingdom.

Lopez, R.S. 1987. The vault sealing program. Proceedings of a Workshop, Toronto, Ont., Atomic Energy of Canada Limited, Pinawa, Man., Technical Report TR339.

Lyon, R.B. 1980. Environmental assessment for nuclear fuel waste disposal — the Canadian program. Atomic Energy of Canada Limited, Pinawa, Man., Technical Report TR-91.

McNamee, J., and Gibson, R.E. 1960. Displacement functions and linear transforms applied to diffusion through porous elastic media. Quarterly Journal of Mechanics and Applied Mathematics, **13**: 98–111.

OECD. 1988. Geological disposal of radioactive wastes: in situ research and investigations in OECD countries. Report prepared by

Nulear Energy Agency Advisory Group, Organization for Economic Cooperation and Development, Paris, France.

Papadopulos, I.S., Bredehoeft, J.D., and Cooper, H.H. 1973. On the analysis of 'slug test' data. Water Resources Research, **9**(4): 1087–1089.

Poon, C.S., Clark, A.I., Perry, R., Barker, A.P., and Barnes, P. 1986. Permeability of Portland cement based solidification process for the disposal of hazardous wastes. Cement and Concrete Research, **6**: 161–172.

Powers, T.C., Copeland, L.E., Hayes, J.C., and Mann, H.M. 1954. Permeability of Portland cement paste. American Concrete Institute Journal, **51**(14): 285–298.

Pusch, R. (*Editor*). 1990. Proceedings OECD Workshop on Artificial Clay Barriers for High Level Radioactive Waste Repositories. Engineering Geology, **28**: 230–462.

Rice, J.R., and Cleary, M.P. 1976. Some basic stress diffusion solutions for fluid-saturated porous media with compressible constituents. Reviews of Geophysics and Space Physics, **14**: 227–241.

Roberts, L.R., and Skalny, J.P. 1989. Pore structure and permeability of cementitious materials. Materials Research Society Symposium, **137**, Boston, Mass.

Rutquist, J. 1995. Determination of hydraulic normal stiffness of fractures in hard rock from well testing. International Journal of Rock Mechanics, Mining Sciences and Geomechanics Abstracts, **32**: 513–523.

Scheidegger, A.E. 1974. The physics of flow through porous media. 3rd ed. University of Toronto Press, Toronto, Ont.

Schlueter, E.M., Cook, N.G.W., Zimmerman, R.W., and Witherspoon, P.A. 1991. Predicting permeability and electrical conductivity of sedimentary rocks from microgeometry. *In* Rock mechanics as a multidisciplinary science. *Edited by* J.C. Roegiers. Balkema, Rotterdam, The Netherlands. pp. 355–364.

Selvadurai, A.P.S. (*Editor*). 1996. Mechanics of poroelastic media. Kluwer Academic Publishers, The Netherlands.

Selvadurai, A.P.S., and Nguyen, T.S. 1995. Computational modelling of isothermal consolidation of fractured porous media. Computers and Geotechnics, **17**: 39–73.

Selvadurai, A.P.S., and Yue, Z.Q. 1994. On the indentation of a poroelastic layer. International Journal of Numerical and Analytical Methods in Geomechanics, **18**: 161–175.

Vaughn, P.J. 1987. Analysis of permeability reduction during flow of heated aqueous fluid through westerly granite. *In* Coupled processes associated with nuclear waste repositories. *Edited by* C.F. Tsang. Academic Press, New York. PP. 529–539.

Watson, G.N. 1944. A treatise on the theory of Bessel functions. 2nd ed. Cambridge University Press, Cambridge, United Kingdom.

White, F.M. 1986. Fluid mechanics. 2nd ed. McGraw-Hill Inc., New York.

Whiting, D., and Walitt, A. (*Editors*). 1988. Permeability of concrete. American Concrete Institute, Skokie, Ill., Publication No. SP108.

Wright, E.D. (*Compiler*). 1991. Semi-annual report of the Canadian nuclear fuel waste management program: October 1, 1990 – March 31, 1991. Atomic Energy of Canada Limited, Report TR-425-10.

Appendix A

The result [10] for the decay of pressure within the cylindrical cavity is applicable only to situations where the outer boundary is located remotely from the pressurized cavity region (eq. [6]). It is therefore necessary to assess the extent to which this assumption can be used to simplify the analysis of the pulse tests conducted on cylinders. In order to address this issue, it is necessary to develop a solution to the pressurized cavity problem where the boundary condition [6] is replaced by the condition:

[A1] $h(b, t) = 0$

where b is the radius of the outer boundary of the cylinder. The details of the solution of the resulting initial value problem are presented elsewhere. Briefly, the differential equation [1] can be rewritten in the non-dimensional form:

[A2] $\tilde{\nabla}^2 \phi = \alpha \dfrac{\partial \phi}{\partial \tau}$

where

[A3] $\tilde{\nabla}^2 = \dfrac{\partial^2}{\partial \rho^2} + \dfrac{1}{\rho}\dfrac{\partial}{\partial \rho}$

[A4] $\rho = \dfrac{r}{a}; \qquad \tau = t\lambda; \qquad \lambda = \dfrac{\pi T_R}{V_w C_w \gamma_w}; \qquad \phi = \dfrac{h}{H_0}$

and α is defined by [11]. By applying the Laplace transform with respect to τ defined by

[A5] $\bar{\phi}(\rho, p) = \displaystyle\int_0^{+\infty} e^{-p\tau}\,\phi(\rho, \tau)\,d\tau$

a general solution of the transformed differential equation [A2] can be obtained. Using the boundary conditions appropriate to the problem of a pressurized cavity in a cylinder with a finite external radius, b, we can obtain a specific solution for $\bar{\phi}(\rho, p)$. The transform inversion of $\bar{\phi}(\rho, p)$ will yield the specific solution for $\phi(\rho, \tau)$. Avoiding details of the analysis, it can be shown that

[A6] $\phi - \phi_\infty = \dfrac{1}{2\pi i}\displaystyle\int_L e^{p\tau}\,(\bar{\phi} - \bar{\phi}_\infty)\,dp$

where $\bar{\phi}_\infty$ is $\phi(\rho, p)$ as $\zeta\ (= b/a) \to \infty$. Considering asymptotic solutions of $\phi(\rho, \tau)$ valid for large ζ and for large τ, it can be shown that

[A7] $\left\{ \left[\dfrac{H(t)}{H_0}\right]_{\zeta \to \infty} - \left[\dfrac{H(t)}{H_0}\right]_{\zeta \to finite} \right\}$

$$\simeq \dfrac{4}{\sqrt{\alpha\tau\pi}}\dfrac{\exp[-\alpha(\zeta - 1)^2/\tau]}{[2 + (\zeta - 1)/\tau]^2} = F(\alpha, \tau, \zeta)$$

It is instructive to evaluate the expression [A7] for the difference in the two expressions for the decay rates, for the experimental configuration involving a typical low permeability material. Considering the experimental configuration and the physical properties of the fluid, we have

$2a = 0.025$ m; $2b = 0.15$ m; $\ell = 0.225$ m.

Hence,

$$\tau = \dfrac{\pi K \ell t}{V_w C_w \mu} \simeq \dfrac{Kt}{a^2 C_w \mu}$$

For

$a^2 \simeq 1.56 \times 10^{-4}$ m^2

$C_w \simeq 4.5 \times 10^{-7}$ m^2

and

$\mu \simeq 10^{-6}$ kN·s/m^2

we have

$$\tau \simeq \frac{Kt \times 10^{17}}{7}$$

where, for consistency, K is expressed in m^2 and t is expressed in seconds. For the range of permeabilities of interest, $K \simeq 10^{-19}$ to 10^{-22} m^2, and for the duration of the test at $t \sim 700$ s, we have $\tau \in (10^{-3}, 1)$. For the experimental configuration and for the material used in the test,

$$\alpha \simeq 0.3; \qquad \zeta = 6 \qquad (\zeta = b/a)$$

Consequently,

(i) for $\tau = 10^{-3}$, $F(\alpha, \tau, \zeta) \to 0$;

(ii) for $\tau = 1$, $F(\alpha, \tau, \zeta) \simeq 1.6 \times 10^{-5}$.

As is evident, the exponential term in [A7] dominates $F(\alpha, \tau, \zeta)$ and appreciable differences in the two solutions will materialize only if $\{\alpha(\zeta - 1)^2/\tau\} \ll 1$. Consequently, for the given experimental configuration involving a low permeability material, the solution derived for the case of the pressure decay within a cavity located in an infinite medium can be used with considerable accuracy for the analysis of the test data. For $\tau \in (10^{-2}, 1)$ and for typical low permeability materials with $K \in (10^{19}, 10^{21})$ m^2, the duration of the test should be limited to approximately 10^3 s.

Figure A1 shows a comparison of the time-dependent decay of pressure within the cavity for the two cases involving

Fig. A1. Pressure decay in a pressurized cylindrical cavity; comparison of solutions.
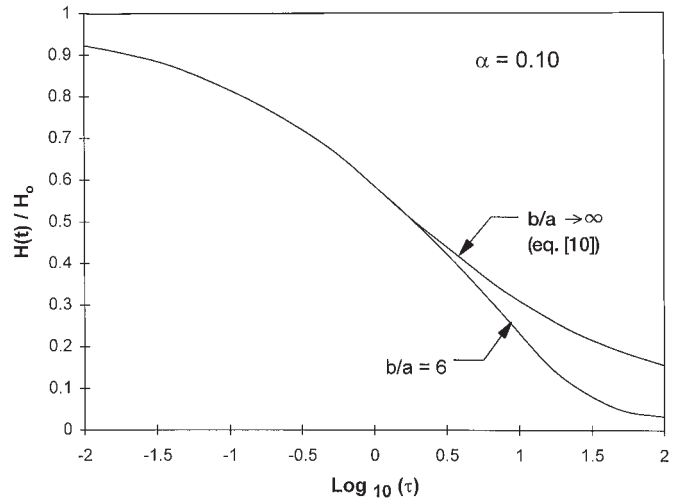
an infinite medium and for a cylinder with a finite outer radius ($\zeta = 6$).